

Reversible Controlled Assembly of Thermosensitive Polymer-Coated Gold Nanoparticles

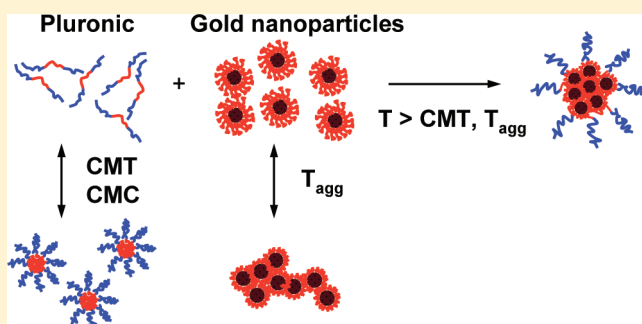
Céline Durand-Gasselín,[†] Nicolas Sanson,^{*,†} and Nicolas Lequeux^{*,†}

[†]Laboratoire de Physico-chimie des Polymères et Milieux Dispersés—Sciences et Ingénierie de la Matière Molle, UMR7615, and

[‡]Laboratoire de Physique et Etudes des Matériaux, UMR8213, UPMC Sorbonne Universités, ESPCI ParisTech, CNRS, Ecole Supérieure de Physique et de Chimie Industrielles ESPCI, 10 rue Vauquelin, 75231 Paris Cedex 05, France

Supporting Information

ABSTRACT: Aggregation of thermosensitive polymer-coated gold nanoparticles was performed in aqueous solution in the presence of a triblock copolymer poly(ethylene oxide)-*block*-poly(propylene oxide)-*block*-poly(ethylene oxide) (Pluronic P123, PEO₂₀-PPO₆₈-PEO₂₀). The gold nanoparticles, AuNPs, which are covered by thermosensitive statistical copolymers poly(EO_{*x*}-*st*-PO_{*y*}), aggregate when the temperature is higher than the phase transition temperature of the polymer, leading to a macroscopic precipitation. The presence of Pluronic chains in solution prevents the uncontrolled aggregation of the AuNPs at higher temperature than both the aggregation temperature of the AuNPs (T_{agg}) and the critical micellization temperature (cmt) of the Pluronic. The size, the colloidal stability, and the optical properties of the AuNPs aggregates are modulated as a function of the P123-to-AuNP ratio, which constitutes the critical parameter of the system. Moreover, the AuNP aggregation is totally reversible upon decreasing the temperature below T_{agg} . Our approach constitutes an easy way to the formation of well-controlled nanoparticle aggregates with well-defined sizes. The resulting aggregates have been characterized by UV-vis spectroscopy, dynamic light scattering, and electron microscopy.



INTRODUCTION

The ability to control the assembly of nanoparticles is a strong concern in many application domains, including biodiagnostics, drug delivery, catalysis, and information storage.¹ The existing methods of assembly are based on electrostatic interactions (metal ion chelation² or complexation³), biospecific recognition (DNA linking⁴ and polymer-based biomolecular recognition⁵), solvophobic interactions,⁶ and multidentate ligands (e.g., multidentate thioethers,⁷ dithiols,⁸ and multifunctional fullerenes⁹). Reversible aggregation of nanoparticles presents a great interest in many application fields as reported in the literature. Methods to achieve such a goal are mainly based on the stabilization of nanoparticles by *stimuli*-responsive polymers, which respond to an external stimulus such as pH, light, or temperature.¹⁰

As a response to the stimulus, water becomes a poor solvent for the polymer chains grafted on the AuNP, therefore leading to the emergence of hydrophobic interactions as the polymer chains undergo conformational changes. Nanoparticle aggregation in aqueous solution induced by these stimuli-responsive polymers generally leads to a macroscopic precipitation without any control of the size and shape of the aggregates and thus represents a difficulty in such systems.

In previous work, we reported the synthesis of dithiol-functionalized thermosensitive polymer-coated gold nanoparticles in aqueous solution.¹¹ The aggregation temperature, T_{agg} , of the AuNPs, which corresponds to the phase transition temperature

of the grafted polymer, can be easily tuned from 8 to 50 °C, both by changing the AuNP size and by increasing the proportion of hydrophilic polymer in the polymer corona. The reversible AuNP aggregation was only driven by the temperature stimulus. However, in all cases, as said above, the aggregation of AuNPs leads to diffusion-limited aggregation and macroscopic phase separation. In aqueous solution, one interesting approach to control the nanoparticle aggregation at a nanoscale level is to govern both short-range attractive and long-range repulsive interactions. In the case of thermoresponsive polymer-coated gold nanoparticles, attractive interactions come from the polymer chains themselves, which become hydrophobic above the phase transition temperature of the polymer. Furthermore, it leads to a macroscopic aggregation due to the absence of long-range repulsive interactions. Then, the control of the nanoparticle aggregation requires the presence in solution of either electrostatic or steric repulsive interactions. In the case of steric repulsions, free copolymer chains in solution, which can both interact with the nanoparticles in solution and maintain a colloidal stability, are well-known in colloid chemistry to act this role. Commercial Pluronic poly(ethylene oxide)-*block*-poly(propylene oxide)-*block*-poly(ethylene oxide), PEO-PPO-PEO, which

Received: June 24, 2011

Revised: September 8, 2011

Published: September 09, 2011

Table 1. Concentrations and Characteristic Temperatures of Gold Nanoparticles and P123 Copolymers Used in This Study

| AuNP@ <i>x/y</i> | nanoparticle concentration (M) | T_{agg} (°C) ^a | P123 solutions (wt %) | cmt (°C) ^b |
|------------------|--------------------------------|-----------------------------|-----------------------|-----------------------|
| AuNP@100/0 | 6×10^{-8} | 12 | 10^{-4} | 36 |
| AuNP@75/25 | 8.5×10^{-8} | 22 | 10^{-3} | 31 |
| AuNP@60/40 | 5×10^{-8} | 38 | 10^{-2} | 26 |
| | | | 10^{-1} | 21 |
| | | | 1 | 16 |
| | | | 5 | 12.5 |

^aThe aggregation temperature (T_{agg}) for AuNP@*x/y* as the function of the DHLA–M600/DHLA–M1000 *x/y* molar ratio is reported in ref 11.

^bThe critical micellization temperature (cmt) of Pluronic P123 aqueous solution as a function of copolymer concentration is indicated and were extracted from data of ref 12, except for values at 10^{-3} and 10^{-4} wt %, which were obtained by extrapolation.

are known to form thermodynamically stable micelles in aqueous solution, possess the required physicochemical characteristics described above to play the role of polymeric surfactant.¹²

In this present work, we report on an original strategy consisting of fine control of the aggregation of polymer-coated gold nanoparticles using Pluronic PEO–PPO–PEO copolymers, which possess the same chemical composition as the polymer grafted on AuNPs. First we demonstrate that the presence of P123 chains prevent the macroscopic phase separation of aggregated AuNPs in solution. Reversible and controlled nanoparticle aggregates are formed in aqueous solution. In the second part of the present work, we highlight the physicochemical parameters allowing one to subtly tune the size of the gold nanoparticle aggregates.

EXPERIMENTAL SECTION

Materials. Amino-terminated poly(ethylene oxide-*st*-propylene oxide), poly(EO-*x-st*-PO-*y*), Jeffamine M600 and M1000, with designed molar masses 600 and 1000 $\text{g} \cdot \text{mol}^{-1}$ and ethylene oxide/propylene oxide, EO/PO, ratio of 1/9 and 19/3, respectively, were purchased from Huntsman Performance Products. Didodecyltrimethylammonium bromide (DDAB), sodium borohydride (NaBH_4), and gold(III) chloride (AuCl_3) were purchased from Alfa Aesar. Tetrabutylammonium borohydride (TBAB), decanoic acid, thioctic acid (TA), 4-(*N,N*-dimethylamino)pyridine (DMAP), *N,N'*-dicyclohexylcarbodiimide (DCC), and poly(ethylene oxide)₂₀-*block*-poly(propylene oxide)₆₈-*block*-poly(ethylene oxide)₂₀ (Pluronic P123, $M_n \sim 5750 \text{ g} \cdot \text{mol}^{-1}$) were purchased from Sigma-Aldrich. All chemicals were used as received.

Synthesis. *Dithiol-Functionalized Thermosensitive Polymers (DHLA–M600 and DHLA–M1000).* Thioctic acid was coupled to Jeffamine M600 and M1000, using DMAP and DCC in CH_2Cl_2 . After purification by chromatographic column, dithiolane-terminated poly(EO-*st*-PO) was reduced into dithiol using NaBH_4 . The ligands denoted DHLA–M600 and DHLA–M1000 were extracted, dried, and then stored under inert atmosphere at 4 °C before used. Details of synthesis are reported in ref 11.

Polymer-Protected Gold Nanoparticles. Six nanometer gold nanoparticles (AuNPs) capped by decanoic acid were prepared by the procedure described in ref 13. Briefly, AuCl_3 (7.5 mg) was dissolved in 1 mL of 100 mM DDAB solution in toluene. Decanoic acid (43 mg) in toluene (2.5 mL) was mixed with the gold salt solution and then TBAB (25 mg) dissolved in 1 mL of DDAB solution was injected to precipitate gold nanoparticles. A ligand-exchange procedure was carried out by mixing AuNPs in toluene (1 mL) with an excess of dithiol-terminated

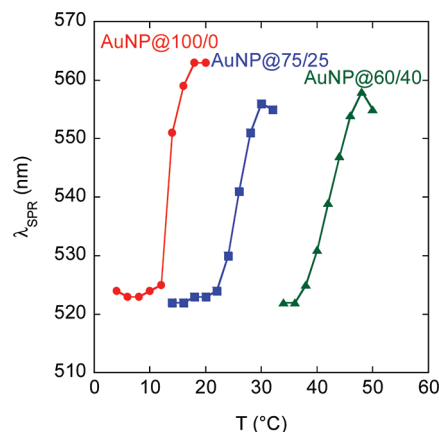


Figure 1. Evolution of maximum wavelength (determined by UV–vis spectroscopy) as a function of the temperature for AuNP@*x/y* in 10 mM KCl solution with different molar ratios DHLA–M600/DHLA–M1000: 100/0, 75/25, and 60/40 (ramp 0.4 °C/min).

Jeffamine as previously reported in ref 11. We used different mixtures of DHLA–M600 and DHLA–M1000 in a 100/0, 75/25, and 60/40 molar ratio. Cap-exchanged nanoparticles were dried, dispersed in ethanol, and purified three times by ultracentrifugation to remove free ligands. After drying, gold nanoparticles were redispersed in 10 mM KCl solution to screen residual electrostatic interactions and stored at ~ 4 °C. The concentration of gold nanoparticles was evaluated using UV–vis absorbance at 400 nm. In the following, polymer-stabilized gold nanoparticles will be labeled AuNP@*x/y*, where *x/y* is the initial DHLA–M600/DHLA–M1000 molar ratio used for the exchange.

Preparation of AuNP and Pluronic Mixtures. Solutions of PEO–PPO–PEO P123 copolymer were prepared in 10 mM KCl solution, ultrasonicated for 15 min at 4 °C, and stored 24 h at low temperature. AuNP solutions were gently mixed with P123 solution, with the temperature kept lower than 4 °C. The final concentrations of gold nanoparticles and the P123 mass percentages in the mixtures are reported in Table 1.

Characterization. *UV–Vis Spectroscopy.* Absorbance measurements were carried out at different temperatures with a UV–vis Hewlett-Packard 8453 spectrophotometer using a quartz cell, in a wavelength ranging from 300 to 900 nm and equipped with a temperature controller (± 0.1 °C).

Microscopy. Transmission Electron Microscopy (TEM) images were performed with a JEOL 2010 field electron gun microscope operating at an acceleration voltage of 200 kV. Samples were prepared by spreading a drop of sample on an ultrathin 300 mesh Formvar/carbon-coated copper grid and dried in air.

Dynamic Light Scattering. Dynamic Light Scattering (DLS) was carried out on a CGS-3 goniometer system equipped with HeNe laser illumination at 633 nm and an ALV/LSE-5003 correlator. All samples were initially filtered through 0.2 μm Millipore syringe filters. The samples were stabilized at constant temperature for 10 min prior to measurement. The data were collected by monitoring the light intensity at a scattering angle of 90°. The hydrodynamic size distribution was obtained using CONTIN algorithm and represented as a percentage of the diffused intensity.

RESULTS AND DISCUSSION

Reversible Aggregation of DHLA–M600/DHLA–M1000-Coated Gold Nanoparticles. At low temperature, all the suspensions of thermosensitive polymer-coated gold nanoparticles present a UV–vis absorption spectrum typical of well-dispersed

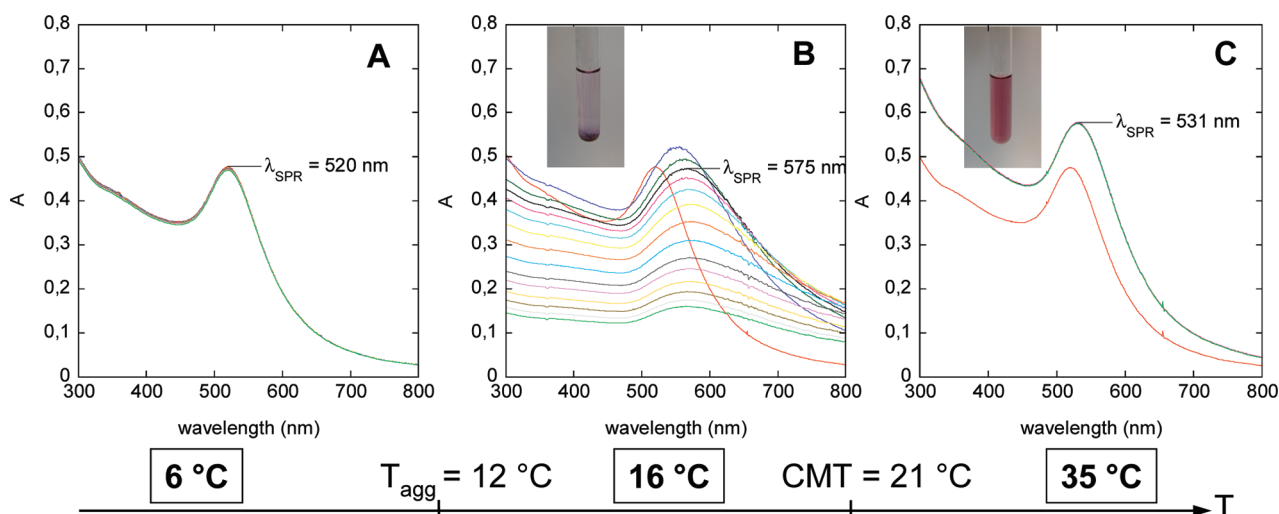


Figure 2. UV–vis kinetics at (A) 6 °C, (B) 16 °C, and (C) 35 °C of AuNP@100/0 ($T_{\text{agg}} = 12$ °C) with 10^{-1} wt % P123 (cmt = 21 °C). UV–vis spectra were recorded every 2 min for 30 min. The red curve was measured at 4 °C before the temperature jump. Inset: pictures of AuNP@100/0 solutions taken after the kinetics.

gold nanoparticles with a characteristic surface plasmon resonance band (SPR) centered at $\lambda_{\text{SPR}} \sim 520$ nm. As the temperature increases, the grafted thermosensitive polymers undergo a phase transition; i.e., they tend to dehydrate and become hydrophobic. Then, at a critical temperature, labeled T_{agg} , an aggregation of AuNPs characterized by a sudden red shift of λ_{SPR} is observed (Figure 1). In a previous study, we have shown that the aggregation mechanism is totally reversible and that λ_{SPR} goes back to the initial value as the temperature decreases below T_{agg} .¹¹ The aggregation temperature depends on the composition of the polymer corona and tends to decrease as the DHLA–M600/DHLA–M1000 ratio increases (see Figure 1 and Table 1). This behavior may be related to the difference of solution properties of both polymers. Indeed, the Jeffamine M1000 is quite similar to pure poly(ethylene oxide), PEO, which is highly soluble in water, even at high temperature, whereas the Jeffamine M600 contains a large fraction of propylene oxide (PO) groups, which are less soluble.¹⁴ The polymer corona behaves as a single statistical poly($\text{EO}_x\text{-st-PO}_y$) copolymer with an intermediate composition leading to a phase transition temperature modulated by the mean EO/PO ratio. As seen in Figure 1, the transition appears smoother for ligand mixtures than for pure DHLA–M600 ligand. This may be related to distribution fluctuation of both grafted ligands from one particle to another.

Influence of the Presence of PEO–PPO–PEO Copolymer Chains on the Stability of AuNP Solutions. One of the main limitations of the nanoparticle assemblies mediated by the temperature stimulus as reported above is that we are unable to control the growth mechanism of nanoparticle clusters (see Figure S1 in the Supporting Information). Beyond T_{agg} , a massive and rapid precipitation of aggregates occurs due to hydrophobization of the grafted polymers on the gold nanoparticle surface. To manage cluster growth, the strategy developed in this work consists of adding surfactant polymer chains into the AuNP suspension, leading to a competition at T_{agg} between nanoparticle–nanoparticle sticking and surfactant–nanoparticle adsorption. The feasibility of this strategy is presented through a first example of solution containing AuNP@100/0 at 6.10^{-8} M

and Pluronic P123 at 10^{-1} wt % (see Figure 2). The mixture was prepared at 4 °C, a lower temperature than the two characteristic temperatures of the system, i.e., the AuNPs aggregation temperature T_{agg} (12 °C) and the expected critical micellization temperature (cmt) (21 °C) of P123 at this concentration (Table 1). Then the solution was quickly brought to a fixed temperature of 6, 16, and 35 °C and characterized by UV–vis absorption spectra recorded every 2 min. At 6 °C, the UV–vis spectra do not evolve with time and there is no apparent sign of aggregation. Indeed, at this temperature, on the one hand, the grafted polymers are well-hydrated and ensure a good dispersion of the gold nanoparticles, and on the other hand, the P123 chains remain as individual unimers in good solvent. When the solution is heated to a temperature between T_{agg} and cmt, the nanoparticles aggregate in an uncontrolled manner and then precipitate (see Figure 2B). Indeed, in this range of temperature, the grafted polymer is mainly in a dehydrated state but the P123 copolymers have not yet started to micellize, assuming a cmt value unaffected by the very low AuNP content. However, Tiberg et al. have shown that the adsorption of PEO–PPO–PEO chains occurs on hydrophobized silica substrate below the critical micellization concentration (cmc).¹⁵ Therefore, it is likely that the P123 chains interact with gold nanoparticles between T_{agg} and cmt, but the surfactant absorbed amount is probably not sufficient to avoid the AuNP aggregation. The process of controlled assembly is only achieved when the temperature is brought beyond T_{agg} and cmt. Indeed, at 35 °C, no macroscopic precipitation takes place (see Figure 2C). In this case, only a slight shift of the λ_{SPR} from 520 to 531 nm is observed during the rise in temperature (~ 1 min) and then spectrum absorbance remains constant. Maintained at 35 °C, these suspensions were found to be very stable over 1 week. Moreover, the absorption spectra are always similar irrespective of the reached final temperature (from 30 to 50 °C). The λ_{SPR} shift and the absence of macroscopic precipitation suggest the formation of limited-size aggregates in the solution during the temperature jump. As described above, the increase of the temperature beyond T_{agg} leads to a hydrophobization of ligands followed by an aggregation. However, as the temperature reaches the cmt of surfactant, the P123 unimers tend to associate

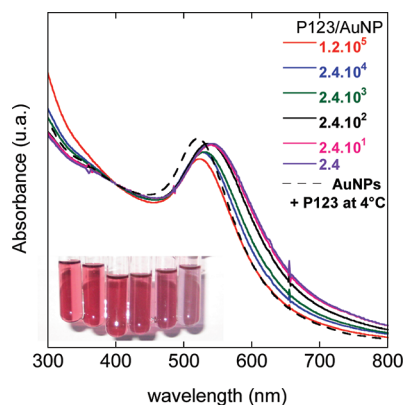


Figure 3. UV–vis spectra of AuNP@100/0 with different concentrations of P123 heated to 40 °C after 30 min, normalized at 400 nm. Inset: picture of the corresponding solutions of AuNP@100/0 with 5, 1, 10^{-1} , 10^{-2} , 10^{-3} , and 10^{-4} wt % P123 from left to right.

to form micelles due to the fact that water becomes a poor solvent for PO groups (hydrogen bonds decrease). Then, the hydrophobic surface of gold nanoparticles behaves as an active surface on which the PPO blocks of the P123 chains condensed.¹⁵ The highly hydrophilic poly(ethylene oxide) blocks, which extend toward the aqueous phase, sterically stabilize the growing AuNP aggregates and thus prevent the gold clusters from noncontrolled macroscopic aggregation. Note that, in addition to the red shift of the surface plasmon resonance band, an increase of the absorbance is also observed, which probably comes from the polymer collapse on the nanoparticle surface that induces an increase of the local refractive index.¹⁶

Tuning Aggregate Size with the Pluronic/AuNP Ratio. As long as the aggregation mechanism is affected by interactions of copolymer chains and AuNPs, it becomes possible to control the size of gold nanoparticle clusters by varying the P123/AuNP ratio. In Figure 3, we show the UV–vis spectra of AuNP@100/0 mixed with P123 solutions at different P123/AuNP ratios from 2.4 to $\sim 120\,000$ measured at 40 °C. This temperature was chosen to ensure the micellization of P123 at all concentrations. For comparison, a spectrum of AuNP solution with P123 chains measured below T_{agg} and cmt is reported in the same figure. As free polymer concentration increases, the shift of λ_{SPR} due to AuNP aggregation tends to decrease. In particular, for the largest P123-to-particle ratio, λ_{SPR} reaches a value very close to that obtained for isolated gold nanoparticles. The shift of λ_{SPR} can also be correlated to the color of the different solutions, which gradually changes from purple to red (see inset in Figure 3) as surfactant concentration increases. The colors together with the absorption spectra of these suspensions do not evolve with time by holding the temperature, suggesting that the system allows a (pseudo)equilibrium state (see Figure S2 in the Supporting Information).

We may anticipate that there is a strong correlation between λ_{SPR} and the aggregate size which are both controlled by the P123/AuNP ratio. To confirm this hypothesis, the aggregate size was investigated by dynamic light scattering. Before studying the aggregates formed from AuNPs and P123 surfactants, we first characterized the hydrodynamic sizes of the different individual components of the system. The hydrodynamic diameters of unimers and micelles of P123 are 4.6 and 19 nm, respectively (see Figure S3 in the Supporting Information), which are in good

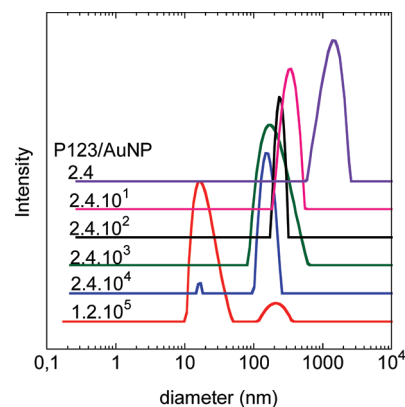


Figure 4. Intensity distribution versus hydrodynamic diameter determined by dynamic light scattering at 40 °C of AuNP@100/0 ($T_{\text{agg}} = 12$ °C) in 10 mM KCl solution with different concentrations of P123.

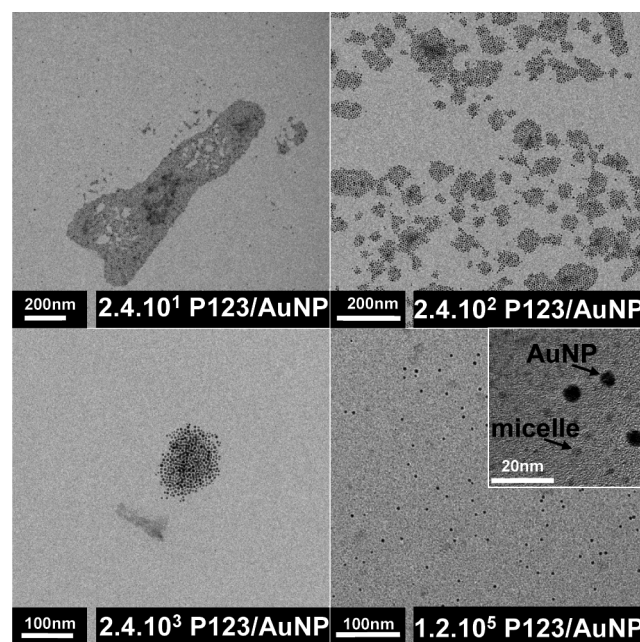


Figure 5. TEM images of AuNP@100/0 aggregates as a function of P123 chains amount in solution.

agreement with reports in the literature.¹⁷ The polymer-coated gold nanoparticles have a hydrodynamic diameter of about 13 ± 1 nm, whatever the nature of the mixture of grafted thermo-sensitive ligands. Intensity distributions of DLS measurements at 40 °C for different P123-to-AuNP@100/0 ratio are reported in Figure 4. For a ratio of 2.4, the distribution is dominated by a unique peak centered at ~ 1300 nm, indicating the presence of a single population of large aggregates. Further, the increase of the free polymer amount leads to a shift of the aggregate sizes toward smaller sizes. This confirms that the size of the gold clusters is well-governed by a competition between the nanoparticle aggregation and the amphiphilic polymer adsorption, which provides a steric stabilization against further aggregation. For the highest P123/AuNP ratio, the DLS intensity distribution exhibits a prominent peak centered at ~ 20 nm and a small secondary peak at 200 nm. However, due to the considerable light diffusion of the largest objects compared to the smallest ones (which

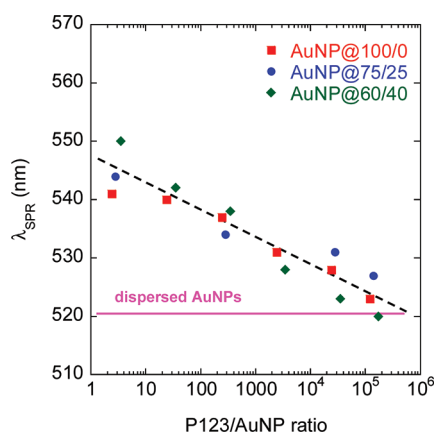


Figure 6. Evolution of the maximum of the surface plasmon band, λ_{SPR} (determined by UV–vis spectroscopy), as a function of the P123 to AuNP ratio, for different AuNP@ x/y .

depends on the power six of the size), the number contribution of the largest population can be neglected. Therefore, DLS data suggest that the sample with high polymer amount contains essentially pure P123 micelles and isolated gold nanoparticles or very small aggregates capped by P123 chains. This conclusion is consistent with UV–vis data, as mentioned above, where a small λ_{SPR} shift between polymer-free AuNP suspension at low temperature and AuNP suspension with high amount of P123 beyond T_{agg} and cmt was observed. The possibility to tune the aggregation from isolated particles to large aggregates with the addition of P123 chains in solution was also confirmed by TEM observations (see Figure 5). For a low P123-to-particle ratio, the observed aggregates are very large and the more abundant the amphiphilic polymer, the more the aggregate size decreases. Note that the aggregate sizes obtained by TEM are consistent with DLS measurements (see Figure S4 in the Supporting Information). However, the TEM size for large clusters is overestimated because of aggregate spreading on the TEM grid during the drying. As expected, for the highest concentration of P123, only individual gold nanoparticles mixed with pure P123 micelles are observed.

The simple method presented above to tune the size of the AuNP aggregates can be generalized to all different thermosensitive polymer-coated gold nanoparticles synthesized in this study. It is important to note that the initial DHLA–M600/DHLA–1000 ratio used for cap-exchange significantly affects the aggregation temperature. Therefore, by varying the nature of grafted polymer and the P123 amount, we can independently modulate the relative position between T_{agg} and cmt. In particular, for AuNP@100/0, T_{agg} is always lower than the cmt of all P123 concentrations between 10^{-4} and 5 wt %, whereas the opposite situation occurs for AuNP@60/40 (see Table 1). For AuNP@75/25, the relative position of T_{agg} in relation to cmt depends on the copolymer concentration. In fact, it is also possible to control the cluster size when cmt is lower than T_{agg} . In those cases no aggregation occurs between cmt and T_{agg} due to the hydrophilic nature of the grafted polymer on nanoparticle surface. An important result is that the cluster sizes only rely on the P123/AuNP ratio but not on the relative values of T_{agg} and cmt. As seen in Figure 6, the values of λ_{SPR} follow a linear relationship with the logarithm of the Pluronic/AuNP ratio, independent of T_{agg} , which is influenced by the composition of

the grafted polymers. Moreover, the cluster sizes determined by DLS are similar for the most part for AuNP@100/0 and AuNP@75/25 at the same P123/AuNP ratios (see Figure S4 in the Supporting Information), meaning that the critical parameter for the control of the AuNP aggregation is the Pluronic-to-AuNP ratio.

On the basis of our observations, it appears that controlled aggregation occurs only when the temperature exceeds the aggregation temperature of the AuNPs and the critical micellization temperature of the P123 copolymer, whatever the relative position of these two critical temperatures. Hecht et al. investigated the micellization kinetics of P123 copolymers and reported that the relaxation time assigned to the association of unimers into a micelle is in the millisecond range.¹⁸ In consequence, it is likely that the temperature jump applied to the mixtures of AuNPs and P123 is slow compared to the micellization process. The surfactant follows an equilibrium state. For a given temperature, at the cmc, the unimer concentration stays constant when the Pluronic concentration increases. If the nanoparticle assemblies were only controlled by the adsorption of unimers on AuNPs surface, the cluster sizes should be independent of the copolymer concentration. It is not the case (see Figure 6). Therefore, our results suggest that the assembly is more controlled by a dissociation equilibrium of surfactants from the micelles to the solution and then to the AuNP surface than the only adsorption of free unimers in solution to the AuNP surface. One another question is about the kinetic differences between nanoparticle aggregation (including dehydration of adsorbed polymer and then aggregation) and surfactant adsorption. From our point of view, the first mechanism is less rapid than the second one. Indeed, as the temperature jump takes more than few seconds, for mixtures with $T_{\text{agg}} < \text{cmt}$, a rapid aggregation mechanism should lead to a macroscopic precipitation before reaching the cmt and should be relatively independent of surfactant concentration. Since the cluster size seems only dictated by the P123/AuNP ratio, we can conclude that the aggregation is a relatively slow process compared to the dissociation kinetics of surfactant from the micelle toward the nanoparticles.

Aggregation Reversibility. As discussed above, the aggregate size can be tailored by manipulating the P123-to-particle ratio and by raising the temperature beyond the aggregation temperature of the AuNPs (T_{agg}) and the cmt. The main originality of our method is that the aggregation mechanism is totally reversed by simply decreasing the temperature below the phase transition temperature of the grafted polymer. By cooling the solution down, λ_{SPR} returns to its initial value around 520 nm, which denotes a complete redispersion of gold nanoparticles. Indeed, as temperature decreases, the thermosensitive grafted polymers reswell (good solvent condition), and spontaneous surfactant-nanoparticle and nanoparticle–nanoparticle separations occur. This reversibility has been experimentally demonstrated by UV–vis spectroscopy during several heating–cooling cycles (see Figure 7). The originality of our system is that both the size and the reversibility of the assembly can be controlled by varying the initial composition of the solution and the temperature.

Thermodynamically Stable Aggregates versus Frozen Aggregates. It is well-known that the PEO–PPO–PEO Pluronics belong to a class of neutral surfactants, able to form thermodynamically stable micelles in water due to a reversible exchange of unimers from the micelles toward the external solution.¹⁹ It is likely that

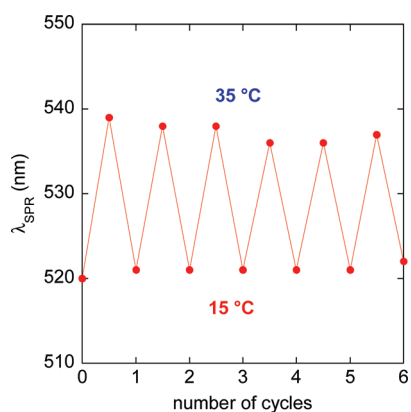


Figure 7. Heating/cooling cycles from 15 to 35 °C in UV–vis of AuNP@75/25 ($T_{\text{agg}} = 22$ °C) mixed with 10^{-1} wt % of P123 (cmt = 21 °C), with a waiting time of 15 min.

this reversibility also occurs in the case of the P123 adsorption onto Jeffamine-capped nanoparticles. Since aggregate sizes result in a mutual compromise between nanoparticle–nanoparticle interaction and the surfactant adsorption, we can question possible exchanges at a constant temperature from one aggregate to the other, leading to an equilibrium state of aggregation. To answer, we started from a state containing aggregates and then we disturbed the system by increasing the total Pluronic P123 concentration without changing significantly both the total solution volume and the AuNP concentration. These experiments were conducted at fixed temperature, and UV–vis spectra were recorded at a regular interval before and after the perturbation (see Figure S5 in the Supporting Information). A rearrangement of the aggregates should induce a blue-shift of the λ_{SPR} due to a decrease of the aggregate size with the P123 amount. In fact, we did not observe a color change even after a long time (several weeks). As expected, to observe the real λ_{SPR} corresponding to the new P123 concentration, the solution needs to be cooled down to 4 °C to redisperse the nanoparticles and then heated again to re-form new smaller aggregates. This experience indicates that rearrangements do not occur and that P123–AuNPs aggregates are frozen assemblies.

CONCLUSIONS

In summary, we have demonstrated an original and simple strategy in order to control nanoparticle assembly. Thermosensitive polymer-coated gold nanoparticles, AuNPs, were mixed with P123 Pluronic chains in solution. We found that reversible controlled aggregates of gold nanoparticles can be achieved in aqueous solution in the presence of Pluronic. Thermosensitive AuNP solutions are not stable when the temperature increases above the aggregation temperature, T_{agg} . By contrast, upon addition of Pluronic chains in solution, the aggregation state and the size of gold nanoparticle aggregates are directly governed by the Pluronic-to-particle ratio. Indeed, the Pluronic chains act as poisons to a macroscopic precipitation of the AuNPs. Our interesting approach presented in this paper is an effortless way to prepare well-defined hybrid micelles controlling the number of gold nanoparticles in the aggregates. Thus, this process can be generalized for various nanoparticles by modifying the anchoring group. We are currently expanding the scope of the control of gold nanoparticle aggregates in the range of high Pluronic concentrations. We anticipate that with subtle mixture of AuNPs

and Pluronic we will enable to finely manipulate smaller AuNP aggregates as dimers or trimers. This work plays a real role in the comprehension of the nanoparticle aggregation mechanism. This simple approach offers great promise for future works in the area of reversible, stable, and controlled-size assembly.

ASSOCIATED CONTENT

S Supporting Information. UV–vis kinetics of AuNPs with different P123 concentrations and DLS of P123 solutions and AuNPs–P123 mixtures. This material is available free of charge via the Internet at <http://pubs.acs.org>.

AUTHOR INFORMATION

Corresponding Author

*N.S.: e-mail, nicolas.sanson@espci.fr; tel, 33 (0) 140 794 417; fax, 33 (0) 140 794 640. N.L.: e-mail, nicolas.lequeux@espci.fr; tel, 33 (0) 140 794 441; fax, 33 (0) 140 794 744.

ACKNOWLEDGMENT

The French Ministry of Research is gratefully acknowledged for funding. We thank Xiangzhen Xu for the TEM images.

REFERENCES

- (1) (a) Grzelczak, M.; Vermant, J.; Furst, E. M.; Liz-Marzan, L. M. *ACS Nano* **2010**, *4*, 3591–3605. (b) Westerlund, F.; Bjornholm, T. *Curr. Opin. Colloid Interface Sci.* **2009**, *14*, 126–134. (c) Romo-Herrera, J. M.; Alvarez-Puebla, R. A.; Liz-Marzan, L. M. *Nanoscale* **2011**, *3*, 1304–1315.
- (2) (a) Zhu, L.; Xue, D. H.; Wang, Z. X. *Langmuir* **2008**, *24*, 11385–11389. (b) Si, S.; Raula, M.; Paira, T. K.; Mandal, T. K. *ChemPhysChem* **2008**, *9*, 1578–1584. (c) Si, S.; Kotal, A.; Mandal, T. K. *J. Phys. Chem. C* **2007**, *111*, 1248–1255. (d) Obare, S. O.; Hollowell, R. E.; Murphy, C. J. *Langmuir* **2002**, *18*, 10407–10410.
- (3) (a) Berret, J. F.; Sehgal, A.; Morvan, M.; Sandre, O.; Vacher, A.; Airiau, M. J. *Colloid Interface Sci.* **2006**, *303*, 315–318. (b) Schneider, G. F.; Decher, G. *Nano Lett.* **2008**, *8*, 3598–3604. (c) Li, C. H.; Hu, J. M.; Liu, T.; Liu, S. Y. *Macromolecules* **2011**, *44*, 429–431.
- (4) (a) Xu, X. Y.; Rosi, N. L.; Wang, Y. H.; Huo, F. W.; Mirkin, C. A. *J. Am. Chem. Soc.* **2006**, *128*, 9286–9287. (b) Alivisatos, A. P.; Johnsson, K. P.; Peng, X. G.; Wilson, T. E.; Loweth, C. J.; Bruchez, M. P.; Schultz, P. G. *Nature* **1996**, *382*, 609–611. (c) Mirkin, C. A.; Letsinger, R. L.; Mucic, R. C.; Storhoff, J. J. *Nature* **1996**, *382*, 607–609.
- (5) (a) Shenhar, R.; Rotello, V. M. *Acc. Chem. Res.* **2003**, *36*, 549–561. (b) Shenhar, R.; Norsten, T. B.; Rotello, V. M. *Adv. Mater.* **2005**, *17*, 657–669. (c) Ofir, Y.; Samanta, B.; Rotello, V. M. *Chem. Soc. Rev.* **2008**, *37*, 1814–1823.
- (6) (a) Yusuf, H.; Kim, W. G.; Lee, D. H.; Aleshyna, M.; Brolo, A. G.; Moffitt, M. G. *Langmuir* **2007**, *23*, 5251–5254. (b) Zhuang, J. Q.; Wu, H. M.; Yang, Y. A.; Cao, Y. C. *J. Am. Chem. Soc.* **2007**, *129*, 14166–14167. (c) Zheng, P. W.; Jiang, X. W.; Zhang, X.; Zhang, W. Q.; Shi, L. Q. *Langmuir* **2006**, *22*, 9393–9396. (d) Poselt, E.; Fischer, S.; Foerster, S.; Weller, H. *Langmuir* **2009**, *25*, 13906–13913. (e) Zubarev, E. R.; Xu, J.; Sayyad, A.; Gibson, J. D. *J. Am. Chem. Soc.* **2006**, *128*, 15098–15099. (f) Selvan, S. T.; Spatz, J. P.; Klok, H. A.; Moller, M. *Adv. Mater.* **1998**, *10*, 132–134. (g) Selvan, S. T.; Hayakawa, T.; Nogami, M.; Moller, M. *J. Phys. Chem. B* **1999**, *103*, 7441–7448. (h) Wang, X. J.; Li, G. P.; Chen, T.; Yang, M. X.; Zhang, Z.; Wu, T.; Chen, H. Y. *Nano Lett.* **2008**, *8*, 2643–2647. (i) Kim, B. S.; Qiu, J. M.; Wang, J. P.; Taton, T. A. *Nano Lett.* **2005**, *5*, 1987–1991. (j) Kamps, A. C.; Sanchez-Gaytan, B. L.; Hickey, R. J.; Clarke, N.; Fryd, M.; Park, S. J. *Langmuir* **2010**, *26*, 14345–14350. (k) Hickey, R. J.; Haynes, A. S.; Kikkawa, J. M.; Park, S. J. *J. Am. Chem. Soc.* **2011**, *133*, 1517–1525.

(7) (a) Maye, M. M.; Luo, J.; Lim, I. I. S.; Han, L.; Kariuki, N. N.; Rabinovich, D.; Liu, T. B.; Zhong, C. J. *J. Am. Chem. Soc.* **2003**, *125*, 9906–9907. (b) Maye, M. M.; Chun, S. C.; Han, L.; Rabinovich, D.; Zhong, C. J. *J. Am. Chem. Soc.* **2002**, *124*, 4958–4959. (c) Maye, M. M.; Lim, I. I. S.; Luo, J.; Rab, Z.; Rabinovich, D.; Liu, T. B.; Zhong, C. J. *J. Am. Chem. Soc.* **2005**, *127*, 1519–1529. (d) Lim, I. I. S.; Vaiana, C.; Zhang, Z. Y.; Zhang, Y. J.; An, D. L.; Zhong, C. J. *J. Am. Chem. Soc.* **2007**, *129*, 5368–5369. (e) Brousseau, L. C.; Novak, J. P.; Marinakos, S. M.; Feldheim, D. L. *Adv. Mater.* **1999**, *11*, 447–449.

(8) (a) Hussain, I.; Wang, Z. X.; Cooper, A. I.; Brust, M. *Langmuir* **2006**, *22*, 2938–2941. (b) Zhang, Y. X.; Zeng, H. C. *Langmuir* **2008**, *24*, 3740–3746. (c) Guarise, C.; Pasquato, L.; Scrimin, P. *Langmuir* **2005**, *21*, 5537–5541.

(9) (a) Brust, M.; Kiely, C. J.; Bethell, D.; Schiffrin, D. J. *J. Am. Chem. Soc.* **1998**, *120*, 12367–12368. (b) Lim, I. I. S.; Pan, Y.; Mott, D.; Ouyang, J.; Njoki, P. N.; Luo, J.; Zhou, S. Q.; Zhong, C. J. *Langmuir* **2007**, *23*, 10715–10724. (c) Lim, I. I. S.; Ouyang, J.; Luo, J.; Wang, L. Y.; Zhou, S. Q.; Zhong, C. J. *Chem. Mater.* **2005**, *17*, 6528–6531.

(10) (a) Si, S.; Mandal, T. K. *Langmuir* **2007**, *23*, 190–195. (b) Nam, J.; Won, N.; Jin, H.; Chung, H.; Kim, S. J. *J. Am. Chem. Soc.* **2009**, *131*, 13639–13645. (c) Tan, J. J.; Liu, R. G.; Wang, W.; Liu, W. Y.; Tian, Y.; Wu, M.; Huang, Y. *Langmuir* **2010**, *26*, 2093–2098. (d) Klajn, R.; Stoddart, J. F.; Grzybowski, B. A. *Chem. Soc. Rev.* **2010**, *39*, 2203–2237. (e) Zhu, M. Q.; Wang, L. Q.; Exarhos, G. J.; Li, A. D. Q. *J. Am. Chem. Soc.* **2004**, *126*, 2656–2657. (f) Shen, Y.; Kuang, M.; Shen, Z.; Nieberle, J.; Duan, H. W.; Frey, H. *Angew. Chem., Int. Ed.* **2008**, *47*, 2227–2230. (g) Cohen Stuart, M. A.; Huck, W. T. S.; Genzer, J.; Müller, M.; Ober, C.; Stamm, M.; Sukhorukov, G. B.; Szleifer, I.; Tsukruk, V. V.; Urban, M.; Winnik, F.; Zauscher, S.; Luzinov, I.; Minko, S. *Nat. Mater.* **2010**, *9*, 101–113.

(11) Durand-Gasselin, C.; Capelot, M.; Sanson, N.; Lequeux, N. *Langmuir* **2010**, *26*, 12321–12329.

(12) (a) Alexandridis, P.; Hatton, T. A. *Colloid Surf., A* **1995**, *96*, 1–46. (b) Alexandridis, P.; Holzwarth, J. F.; Hatton, T. A. *Macromolecules* **1994**, *27*, 2414–2425.

(13) Jana, N. R.; Peng, X. G. *J. Am. Chem. Soc.* **2003**, *125*, 14280–14281.

(14) Aseyev, V.; Tenhu, H.; Winnik, F. M. *Adv. Polym. Sci.* **2011**, *242*, 29–89.

(15) Tiberg, F.; Malmsten, M.; Linse, P.; Lindman, B. *Langmuir* **1991**, *7*, 2723–2730.

(16) Contreras-Caceres, R.; Sanchez-Iglesias, A.; Karg, M.; Pastoriza-Santos, I.; Perez-Juste, J.; Pacifico, J.; Hellweg, T.; Fernandez-Barbero, A.; Liz-Marzan, L. M. *Adv. Mater.* **2008**, *20*, 1666–1670.

(17) (a) Ganguly, R.; Kumbhakar, M.; Aswal, V. K. *J. Phys. Chem. B* **2009**, *113*, 9441–9446. (b) Newby, G. E.; Hamley, I. W.; King, S. M.; Martin, C. M.; Terrill, N. J. *J. Colloid Interface Sci.* **2009**, *329*, 54–61.

(18) Hecht, E.; Hoffmann, H. *Colloid Surf., A* **1995**, *96*, 181–197.

(19) (a) Zana, R.; Marques, C.; Johner, A. *Adv. Colloid Interface Sci.* **2006**, *123*, 345–351. (b) Nicolai, T.; Colombani, O.; Chassenieux, C. *Soft Matter* **2010**, *6*, 3111–3118. (c) Denkova, A. G.; Mendes, E.; Coppens, M. O. *Soft Matter* **2010**, *6*, 2351–2357.